International Journal of Hydrogen Energy 220 (2026) 154042

Contents lists available at ScienceDirect

International Journal of Hydrogen Energy

journal homepage: www.elsevier.com/locate/he

Development of a sieverts-type apparatus with enhanced automation using a dual-valve pressure control device for solid state hydrogen storage applications

Julián Arias [a,*], Robinson Aguirre-Ocampo [a], Joan Santiago Cortinez [a], Carlos Arrieta [b], Francisco Bolivar [a], Alejandro Zuleta [d], José A. Tamayo [e], Andrés F. Vargas [f], Esteban Correa [c], Félix Echeverria [a]

[a] Centro de Investigación, Innovación y Desarrollo de Materiales - CIDEMAT, Facultad de Ingeniería, Universidad de Antioquia UdeA, Calle 70 No. 52-21, Medellín, 050010, Colombia
[b] Grupo de Investigación en Energía – GRINEN, Facultad de Ingenierías, Universidad de Medellín UdeM, Carrera 87 No 30 – 65, Medellín, Colombia
[c] Grupo de Investigación Materiales con Impacto – MAT&IMPAC, Facultad de Ingenierías, Universidad de Medellín UdeM, Carrera 87 No 30 – 65, Medellín, Colombia
[d] Grupo de Investigación de Estudios en Diseño - GED, Facultad de Diseño Industrial, Universidad Pontificia Bolivariana, Sede Medellín, Circular 1 No 70 – 01, Medellín, Colombia
[e] Grupo de Materiales Avanzados y Energía-Matyer, Instituto Tecnológico Metropolitano - ITM, Medellín, Colombia
[f] Grupo Química Básica, Aplicada y Ambiente - Alquimia, Facultad de Ciencias Exactas y Aplicadas, Instituto Tecnológico Metropolitano, Medellín, Colombia

ARTICLE INFO

Keywords:
Automation in hydrogen storage testing
Gas dosing automation
Sieverts-type apparatus design
Pressure management
Inlet/outlet control

ABSTRACT

High-pressure volumetric sorption analyzers, commonly referred to as Sieverts-type apparatuses, offer precise measurements of absorption capacity, kinetics, pressure-composition isotherms (PCI), thermodynamic properties, and cyclic stability for materials utilized in hydrogen storage research. Although advanced commercial systems are available, their design or cost often limits measurement flexibility or accessibility, prompting many research groups to develop their self-built alternatives. However, achieving precise gas pressure/flow control, as well as complete automation, remains a challenge, as existing methods often require manual intervention and present opportunities for further optimization. This study tested a novel integration of a Pressure Control Device (PCD) into a self-built Sieverts-type apparatus, aiming to automate key aspects of hydrogen dosing and pressure control in hydrogen absorption measurements. The PCD was incorporated into the design and subsequently assembled. The system was volume-calibrated and used to evaluate the hydrogen storage capacity, kinetics, PCI, and cyclic stability of a known composite material consisting of commercial MgH_2 powder (>98% purity) doped with 1 wt% commercial carbon-coated nickel nanoparticles. Additional kinetic and cycling stability tests were conducted using $LaNi_5$ to demonstrate the system's applicability to different classes of metal hydrides. Our test proved to be a viable and cost-effective alternative for retrofitting self-built systems, facilitating the measurement of hydrogen-absorbing materials. Integrating a PCD streamlines measurement operations, improves reproducibility, and reduces manual handling and other time-consuming tasks.

1. Introduction

High-pressure volumetric sorption analyzers, also known as Sieverts-type apparatuses, have significantly contributed to our current understanding of hydrogen-absorbing materials for energy storage applications over the past few decades. While not the only tools capable of measuring absorption capacity, kinetics, Pressure-Composition Isotherms (PCI or PCT), thermodynamic parameters, temperature-programmed desorption, and cyclic stability, Sieverts-type systems are the most widely used due to their relatively low cost, ease of operation,

* Corresponding author. Calle 70 No. 52, Medellín, 050010, Colombia.
E-mail addresses: juliariasvelandia@gmail.com, tramites.cidemat@udea.edu.co (J. Arias), robinson.aguirre@udea.edu.co (R. Aguirre-Ocampo), joan.cortinez@udea.edu.co (J.S. Cortinez), Carrieta@udemedellin.edu.co (C. Arrieta), francisco.bolivar@udea.edu.co (F. Bolivar), alejandro.zuleta@upb.edu.co (A. Zuleta), josetamayo@itm.edu.co (J.A. Tamayo), andresvargas@itm.edu.co (A.F. Vargas), escorrea@udemedellin.edu.co (E. Correa), felix.echeverria@udea.edu.co (F. Echeverria).

https://doi.org/10.1016/j.ijhydene.2026.154042
Received 14 August 2025; Received in revised form 7 January 2026; Accepted 11 February 2026
Available online 21 February 2026

and reliable performance for laboratories and researchers.

The significance of Sieverts-type apparatuses in hydrogen storage research is well-established, with over 1300 papers documenting their use. The steady flow of publications since 2002, along with high citation rates, underscores their centrality in the field, serving as a reference for both academic and industrial studies. Commercial Sieverts-type systems dominate the literature, often serving as benchmarks for precision and reliability. The wide range of commercial offerings reflects researchers' trust, as they cite commercial references significantly in the literature. Five hundred seventeen scientific articles mention eleven references to devices manufactured in the United States, France, Japan, Germany, China, and the United Kingdom, which include, in addition to their basic parts, accessories like mass flow meters for dynamic PCT measurements, and spectrometers, or thermal conductivity detectors to enhance a TPD measurement. Appendix A of the Supplementary Material contains a list and citations of 14 commercial references to Sievert-type apparatuses and their principal capabilities, as identified in our review of the open internet.

Researchers' trust in commercial equipment is supported by the manufacturers' efforts to present integrated and compact systems with all the functionalities and software that impact the accuracy of test results. Post-sale support, maintenance, and spare parts availability also provide reassurance. While these systems are advanced, the costs (80,000 – 200,000 USD) or specific research requirements, drive many research groups to develop self-built apparatuses focusing on affordability and customization. These setups frequently operate within similar temperature and pressure ranges as commercial units. Still, notable innovations include the integration of mass flow meters [1], cryogenic temperature capabilities [2], and improvements in volume calibration techniques [3]. Despite the diversity in designs, the core functionality of these systems remains similar to commercial counterparts, with enhancements often geared toward improved sensitivity and error minimization.

Researchers who opt to build their Sieverts-type apparatuses often seek full automation to handle the time-intensive nature of hydrogen absorption tests. Automation typically involves creating a programmable sequence of pressure and temperature variations, enabling the equipment to autonomously execute experiments, record the resulting data, and make data available for analysis. Despite various gas flow or dosing control methods in the literature, details are often sparse. Some setups rely on self-developed software for pressure management [4], while others use pneumatic regulators or on/off pneumatic valves combined with micrometric valves [5], requiring unavoidable manual adjustments. More advanced systems incorporate flow meters to automate cutoff based on pressure sensors [6], or syringe pumps for precise gas dosing [7]. However, the use of a dual-valve Pressure Control Device (PCD) or Electronic Pressure Regulator (EPR) remains undocumented in the scientific open literature. These devices, which resemble flow meters, feature three channels: one for gas entry, another for flow control to the sample cell, and a third for venting, allowing precise pressure management. Manufacturers, such as *Alicat Scientific* (Tucson, AZ) and *Equilibar* (Fletcher, NC), offer advanced solutions specifically designed to optimize the filling of closed volumes under controlled conditions. The latter, Equilibar, is more cost-effective.

The primary objective of this study is to document a comprehensive test of material for hydrogen storage applications (capacity, kinetics, PCI, and cycling) using a self-built Sieverts-type apparatus incorporating a PCD, thereby evaluating the feasibility of this instrument in enhancing automation and efficiency in hydrogen absorption measurements.

2. State of the art

Over recent decades, the Sieverts technique has seen considerable refinement, driven by the need to better characterize hydrogen absorption properties in various materials [8,9]. Researchers who have opted to build their apparatuses have expanded their use, applying it to low-density and porous materials, such as carbon nanotubes [7,10,11]. One focus has been enhancing measurement accuracy through innovative methods such as dual-channel systems and advanced thermal compensation using differential pressure (ΔP) approaches [3,12].

Table 1 presents some of the most representative automated self-building equipment found in the literature. Most are designed to operate at temperatures above 300 °C, although some can function across a wide range of temperatures. A few devices have been reported to operate at low temperatures, close to 77K. Working pressures typically range from 3 to 10 MPa, with equipment designed for small volumes usually not exceeding 15 mL. Despite these differences, the various apparatuses show the efforts of researchers to achieve good sensitivity, measuring with precision and reproducibility.

Sieverts-type apparatuses summarized in Table 1 also reveal the absence of documented implementations of Pressure Control Devices (PCDs) or Electronic Pressure Regulators (EPRs) for automating hydrogen inlet and outlet in the measurement processes. Current self-built systems predominantly rely on conventional mechanisms, such as needle valves, mass flow controllers (MFCs), and manual or semi-automated dosing configurations. These setups, often integrated with custom software or gas bottle systems for applications like PCI analysis.

Provide basic control but are constrained by their dependency on manual adjustments and limited precision. The lack of advanced automation in these configurations underscores the need for innovations that improve operational efficiency, reproducibility, and user accessibility in hydrogen storage research.

3. Design and assembly

Fig. 1 presents the P&ID, mechanical layout, and a photograph of the custom-built Sieverts-type apparatus. The system was designed to operate under controlled pressures ranging from 0 to 100 bar and temperatures between 20 and 450 °C.

The instrumentation includes a dual-valve pressure controller (ALICAT PCD-1000PSIG-D-485-PCA13/5P, Tucson, AZ), which regulates hydrogen dosing and venting up to 100 bar with an accuracy of ±0.25% of full scale (labeled PIC in Fig. 1). Pressure measurements are provided by a high-precision Keller pressure transducer (PA-33X, Winterthur, Switzerland), offering a range of 0–100 bar and an accuracy of ±0.05% full scale (PIT in Fig. 1). Two custom-designed ovens control the temperature of key volumes in the system. Oven Z-I regulates the sample cell volume (V_{sc}) over a range of 20–450 °C with ±2 °C precision, while oven Z-II controls the reference volume (V_{ref}) within a range of 20–150 °C and a precision of ±1 °C. Temperature monitoring is achieved using a K-type thermocouple (TIC-1) for V_{sc} and a PT-100 resistance temperature detector (RTD, TIC-2) for V_{ref}.

The system's instrumentation is fully integrated into a Siemens S7-1200 PLC (model 1214C, Munich, Germany), which serves as the central control unit. Communication between the programmable control device (PCD) and the Keller pressure transducer is achieved via Modbus RTU protocol over an RS485 serial network, with a Siemens CB-1241 communication module acting as the master. Temperature control subsystems are connected to the PLC via analog inputs (0–10 V) interfaced through the Siemens SM1222 module, whose transistor-type digital outputs drive solid-state relays (SSRs) to regulate power supply to the heaters. A self-tuning Siemens PID algorithm enables precise and stable temperature control during experiments, dynamically adjusting output response to compensate for load variations and thermal inertia.

The control program, developed using Siemens TIA Portal V17, includes modular routines for closed-loop temperature regulation, continuous hydrogen pressure monitoring, and manual valve actuation. In addition to basic operation, several automated control modes have been implemented to support specific experimental procedures (e.g., capacity measurements, PCI curves, and kinetic tests); these will be detailed in later sections. Although more advanced dosing strategies have been reported in the literature, such as real-time adjustment of

Table 1
Pressure control, dosing, and general features of self-built sieverts-type apparatuses (2006-present).

Authors	Year	Reactor volume	*P* (MPa)	*T*(K)	Mass flow metre	Channels	Main Capabilities	Novelty	Pressure control and dosing	Ref
Meyer et al.	2007	NR	6	823	No	Single	Cycling	Cycling automatization with self-hydrogen generation	Not applicable	[13]
Zielinski et al.	2007	<50 mL	2	1023	No	Double	PCT	Differential pressure measurements	The device, though unmentioned, had programmable pressure settings controlled by a load file.	[4]
Talagañis et al.	2009	~8 mL	6	723	Yes	Single	PCT and phase determination	Thermal desorption spectroscopy combined with XRD	The device, though unmentioned, had programmable pressure settings controlled by self-developed software	[14]
Voskuilen et al.	2010	15 mL	70	240 - 320	No	Single	PCT and kinetics	Multiple transducer configuration	High-pressure pneumatic regulator linked to control software, with no specific details provided.	[15]
Policicchio et al.	2013	5.8 mL	8	77 - 470	Yes	Single	PCT and kinetics	Minimizes the sources of systematic errors in the method	A MFC controls gas inlet, while transducers monitor the pressure.	[6]
Lim et al.	2015	9 - 19 mL	4	873	No	Double	PCT and Cycling	Channel independently operated modifying sensitivity	Controlled by a pneumatic on/off diaphragm valve, a needle valve, and the pressure transducer	[5]
Pyle et al.	2017	12 mL	30	77 - 873	No	Single	PCT	Low-density materials where the sample volume has uncertainty	A linear piston pump boosts and controls hydrogen pressure, managed by a piston control unit linked to the PC	[7]
Ceteroni et al.	2019	~12 mL	10	77-298	No	Double	PCT	Impact of valve volume and double channel on accuracy.	Controlled by a pneumatic on/off Bellow-Sealed Valves, a needle valve, and the pressure transducer	[16]
Testi et al.	2020	40 mL	4	~650	No	Double	PCT and kinetics	Uncertainty reduction by isochoric differential pressure sensing	The device, though unmentioned, had programmable pressure settings controlled by a load file.	[17]
Zhu et al.	2022	~3 mL	10	1073	No	Single	PCT, kinetics and cycle	Compact design and automatic dosing with volume enlargement	Exclusive for PCI analysis using gas bottles and valves incorporated into the system.	[18]
Zhu et al.	2024	~11 mL	10	1073	No	Single	PCT, kinetics and cycle	TCV testing and methods for volume calibration	Exclusive for PCI analysis using gas bottles and valves incorporated into the system.	[3]

hydrogen dosing based on the instantaneous absorption rate of the material, the development and validation of such adaptive control algorithms were beyond the scope of the present work. Nevertheless, the proposed hardware–software architecture has been intentionally designed to be fully compatible with real-time adaptive and feedback-based dosing strategies, which can be readily incorporated in future developments.

Data acquisition is performed using a custom Python script that utilizes the Snap7 library, enabling reliable bidirectional communication with the PLC via the S7 protocol and storing experimental data (such as pressure and temperature) in a CSV file for further analysis and visualization. To support real-time process monitoring, a built-in PLC web server provides live access to the system's variable table through any browser-enabled device. For enhanced usability, a Python-based graphical user interface (GUI) was developed using the Tkinter library, offering live pressure visualization to facilitate experimental supervision and on-the-fly adjustments. Fig. 2 presents a schematic diagram of the technological architecture for integrating hardware, control, and data acquisition in the apparatus development.

The pressure vessels and tubing in the system were selected in 316L stainless steel for its excellent corrosion resistance and mechanical strength. This material supports working pressures of up to 124 bar. The system's two key volumes consist of V_{sc}, with an internal nominal volume of 9 mL, and V_{ref}, with 150 mL. The V_{sc} was machined from a solid rod and welded to a VCR short tube butt weld gland, ensuring a compact and leak-tight design. In contrast, the V_{ref} corresponds to a commercial Swagelok sample cylinder, offering precise capacity and compatibility with high-pressure applications. Airtight sealing, particularly adjacent to heating zones, is achieved using Swagelok VRC-type connections, ensuring leak-free performance under cyclic thermal and pressure loads. Although the present study was conducted using a fixed reactor and reference volumes, the system was intentionally designed with a modular, laterally arranged architecture that allows straightforward replacement or resizing of both the sample cell and the reference volume. This inherent flexibility enables the setup to be adapted to different material types, sample masses, or precision requirements, thereby addressing the need for variable chamber sizes in advanced hydrogen storage studies.

Thermal insulation and heat management were carefully considered in the system layout to ensure stable and reproducible high-temperature operation. The lateral arrangement of the sample cell and reference volume facilitates the installation of localized thermal insulation around the heated zones, minimizing heat losses and reducing thermal gradients along the connecting lines. High-temperature insulation materials were applied around the sample cell and furnace region, while thermal breaks and spatial separation were used to limit heat transfer to sensitive components. Maintaining consistent insulation conditions during volumetric calibration and experimental testing was prioritized, as variations in heat loss can directly affect gas temperature and density and, consequently, measurement accuracy.

Safety considerations in hydrogen handling were an integral part of the system design and operation. A portable hydrogen leak detector (KP810 single gas detector, Henan Zhongan Electronic Detection Technology Co.) was routinely used for local leak inspection during assembly, commissioning, and experimental operation. This device operates based on catalytic/electrochemical sensing principles and provides a detection range of 1–100 ppm, enabling early identification of minor hydrogen leaks. In addition, the hardware architecture of the system allows the integration of fixed hydrogen sensors with lower sensitivity directly into the control framework, enabling digital interlocks that can

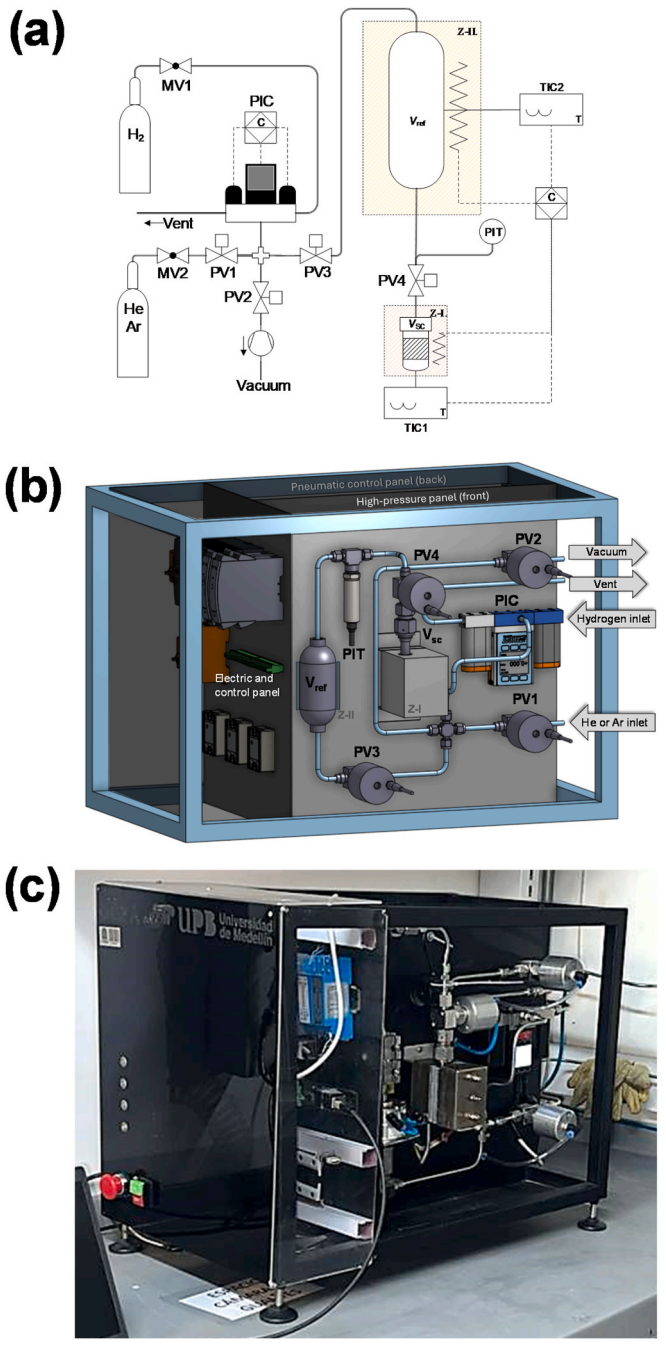

Fig. 1. Schematic representation of the self-built Sieverts-type apparatus with enhanced automation using a dual-valve Pressure Control Device (PCD).

automatically interrupt operation and drive the system to a safe state in the event of abnormal hydrogen levels. Overpressure protection is ensured through dedicated pressure relief valves installed at critical points of the system, which are specified according to the maximum allowable working pressure of each subsystem. Together, these measures provide multiple layers of protection, including early leak detection, automatic shutdown capability, and mechanical pressure relief, ensuring safe operation during high-pressure hydrogen experiments.

During basic test operation, initial gas pressures are manually adjusted via manual valves MV1 and MV2. Fine pressure control, dosing, and venting are handled downstream by the PCD. Gas is distributed throughout the system via ¼-inch tubing and directed by pneumatically actuated valves (SS-HBVCR4-C, Swagelok) identified as PV1–PV4. PV1 manages the purge gas inlet used in the calibration of V_{sc}; PV2 connects the system to a Robinair vacuum pump (model 15500, Plymouth, MI), capable of achieving pressures as low as 30 mbar, enabling complete evacuation prior to hydrogen exposure; PV3 and PV4 control the internal flow paths between the V_{ref} and V_{sc}, enabling isolation, equilibration, or transfer operations as dictated by the test protocol. The pneumatic valves are energized through solenoid actuators that are controlled by relay-type digital outputs from the PLC. A standard air compressor operating above 5.5 bar supplies the compressed air required for actuation. The modular architecture and clear valve logic enable both manual and automated gas flow configurations, allowing for flexible sequencing of tasks such as evacuation, gas dosing, equilibration, and desorption. Table B1 in Appendix B of the Supplementary Material presents a list of parts and prices that we spent on the development.

4. Materials and methods

Magnesium hydride powder (≥98% purity) was obtained from Lead Optima Element Tech Co., while carbon-coated nickel nanoparticles (C@Ni) with a purity of ≥99.9% were sourced from Nanostructured & Amorphous Materials. LaNi doped with Ce and Co, was obtained from Hefei Sinopower Technologies Co., Ltd. All sample preparation was carried out inside an argon-filled glovebox (Vigor Tech USA), maintaining oxygen and moisture levels below 1 ppm to prevent contamination. High-energy ball milling was performed using a Retsch Emax mill with stainless steel jars coated in ZrO_2. The MgH_2 powder was milled at 800 rpm using 3 mm diameter ZrO_2 balls in a 125 mL ZrO_2-coated stainless steel jar. Milling was conducted with a ball-to-powder weight ratio of 80:1 and a 50% vial filling volume. The total milling duration was 1 h, divided into alternating cycles of 10 min of milling followed by 10 min of cooling to prevent overheating. Carbon-coated nickel nanoparticles were incorporated at a 1 wt% concentration relative to the MgH_2 powder during the ball milling process, as reported in previous work [19]. A ThermoFisher Scientific Apreo 2 field emission scanning electron (FESEM) microscope was employed for morphological characterization.

For volume calibration, we employed the known displacement volume calibration sample method [20], wherein the apparent volumes (corrected for thermal expansion effects) are estimated using the continuity equation that equates the number of moles of gas before and after decompression in tests conducted with and without a piece of known volume inside the V_{sc}. A total of 25 expansion cycles were performed while maintaining the V_{ref} at a constant temperature of 100 °C. During these experiments, the PCD was used to set five discrete pressure levels (0.5, 1.0, 1.5, 2.0, and 2.5 MPa) within the system, and V_{sc} was set at five different temperatures: 150 °C, 200 °C, 250 °C, 300 °C, and 350 °C. The pieces of known volumes were three precision-machined stainless-steel spheres, each with a diameter of 0.463 cm, weighing 414.4 mg and having a volume of 0.0518 cm^3. The primary objective of these calibration tests was to validate the accuracy and responsiveness of the PCD across the specified temperature range, obtaining sufficient data to generate reliable temperature-dependent volume calibrations for V_{ref}. The calibrated volume was then used to determine the hydrogen desorption profile of 380.2 mg of $LiAlH_4$ (>97% purity, Merck, Germany), which was employed as a reference material.

The V_{sc} was subsequently charged with 208.7 mg of the material inside the argon-filled glovebox. For the kinetic experiments, hydrogen absorption was performed at an initial hydrogen pressure of 2.1 MPa. Desorption kinetics were evaluated under an initial vacuum pressure of 0.0025 MPa. After each kinetic measurement at 350 °C, 300 °C, and 275 °C, the sample was fully rehydrogenated or dehydrogenated at 375 °C before proceeding to the following test condition, ensuring consistent initial states for each experiment.

For the temperature-programmed desorption (TPD) analysis, the same sample was first fully hydrogenated at 375 °C. Following hydrogenation, the system was cooled down to 100 °C. With the valve PV4

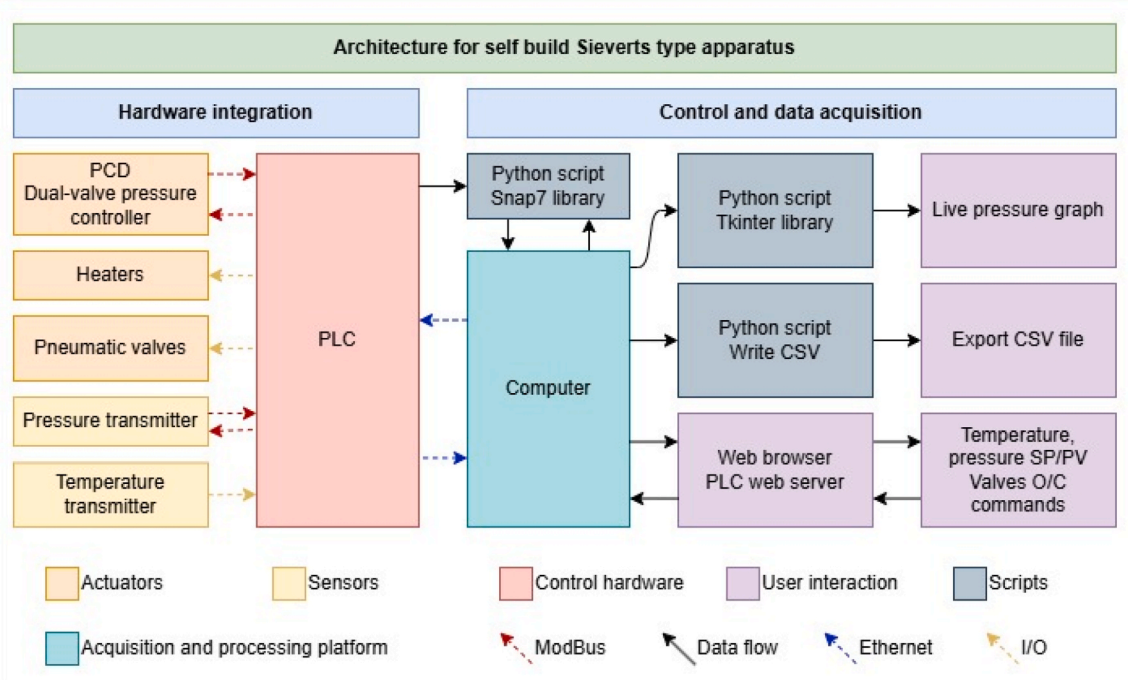

Fig. 2. Technological architecture and data flow of the self-built Sieverts-type apparatus with enhanced automation, integrating a dual-valve pressure control device (PCD), PLC-based control hardware, and Python-based data acquisition.

open, the pressure was reduced to 0.0025 MPa using the vacuum pump to establish desorption conditions. Subsequently, the sample was subjected to a linear temperature ramp of 5 °C/min from 100 °C to 400 °C, and the evolved hydrogen was monitored throughout the heating process.

Cyclic hydrogen absorption/desorption tests were performed by first fully hydrogenating the sample at 2.1 MPa and 350 °C for 2 h. Ten cycles were then conducted, with absorption at 2.1 MPa and desorption under a vacuum of 0.0025 MPa. During cycling, temperatures were maintained at 100 °C in the reference volume (V_{ref}) and 350 °C in the sample cell (Vsc). This protocol evaluated the material's capacity retention and reversibility under repeated cycling. Additionally, following reviewers' suggestions, an extended cycling test comprising 70 absorption/desorption cycles was conducted using $LaNi_5$, a material with lower hydrogen storage capacity but well-known low-temperature operating characteristics, to demonstrate the system's functionality with a different class of hydrides. These cycles were performed under the same pressure conditions (2.1 MPa for absorption and 0.0025 MPa for desorption) at 25 °C for both V_{ref} and V_{sc}.

Pressure–composition isotherm (PCI) tests were conducted at 350 °C on the same sample. After complete dehydrogenation, hydrogen absorption was measured at 10 pressure set points, programmed using the PCD; subsequently, desorption was evaluated at 11 decreasing pressures, starting from the final absorption condition. Unlike the cyclic tests, the system was not evacuated between steps, enabling continuous, isothermal measurement of hydrogen uptake and release as a function of pressure.

The equations and calculation models used for data analysis are documented in the accompanying Python notebooks, which are accessible through hyperlinks provided in the Results section. For numerical operations and data management, the analysis relied on the NumPy and Pandas libraries, while Matplotlib was employed for data visualization. Elemental properties were accessed using the PeriodicTable library, and thermodynamic properties such as the compressibility factor were calculated using CoolProp. The core equations implemented in these workflows are based on the models reported by Webb and ray (2014) [21] Zhu et al. (2022) [18]¶ and Carrillo-Bucio et al. (2018) [12].

The uncertainty analysis was conducted in accordance with the Guide to the Expression of Uncertainty in Measurement (GUM), taking into account all relevant sources of experimental error, including sensor accuracy, instrumental resolution, calibration procedures, valve dead volume, and potential system leaks. The amount of hydrogen absorbed, n, and its associated uncertainty were calculated from the measured pressure (P), temperature (T), volume (V), gas constant (R), and compressibility factor (Z) using Eqs. (1) and (2):

$$n = \frac{PV}{ZRT}, \tag{1}$$

$$\frac{u^2(n)}{n^2} = \left(\frac{u(P)}{P}\right)^2 + \left(\frac{u(T)}{T}\right)^2 + \left(\frac{u(V)}{V}\right)^2 + \left(\frac{u(Z)}{Z}\right)^2 + \left(\frac{u(R)}{R}\right)^2, \tag{2}$$

where u represents the standard uncertainty associated with each variable. For pressure and temperature, uncertainties were obtained directly from the specifications and calibration certificates of the pressure transducers and thermocouples installed in the system, yielding ±0.05 bar for pressure and ±1 K for temperature. These values include both sensor accuracy and signal conditioning contributions. The uncertainty in volume was derived from the volumetric calibration of the reference and sample cells, which inherently accounts for valve deadspace and internal tubing volume. The compressibility factor Z was calculated from Leachman et al. equation for hydrogen (based on Helmholtz free energy) under the measured pressure and temperature conditions, and its uncertainty was propagated accordingly. The gas constant R was taken from NIST with a reported relative uncertainty of 9.1×10^{-7}. In addition, system integrity was verified through leak tests and pressure decay tests prior to experimental runs, ensuring that leakage contributions were negligible within the measurement time scale.

5. Results

Fig. 3 presents the SEM images, which reveal a uniform distribution of carbon-coated nickel (C@Ni) nanoparticles throughout the magnesium hydride (MgH_2) matrix. The as-received commercial MgH_2 exhibits an average particle size of approximately 8 μm, while the carbon-coated

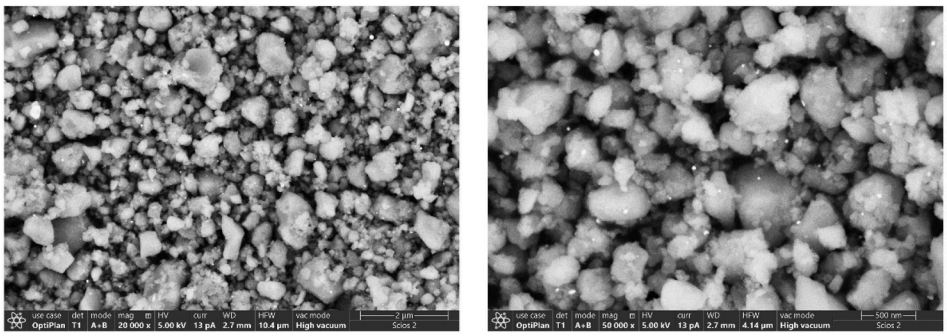

Fig. 3. SEM images of MgH_2–1 wt% C@Ni composite, illustrating nanoparticle distribution and post-milling morphology.

nickel nanoparticles have a characteristic diameter of less than 40 nm. Following the high-energy ball milling and mixing process, a significant reduction in particle size is observed, with the majority of the composite particles measuring less than 1 μm.

The procedure for calculating apparent system volumes from calibration measurements is presented in the Python notebook "Calibration_MS-PCD.ipynb," accessible via the provided hyperlink. Solving the calibration equations for 25 expansion experiments yielded apparent volumes of 169.2 mL for V_{ref} and 5.7 mL for V_{sc}, corresponding to a V_{sc}/V_{ref} ratio of 0.034. The standard deviation of this ratio, calculated across different temperature datasets, was 0.0025. These calibrated volumes were subsequently employed to quantify the dehydrogenation of $LiAlH_4$, resulting in a measured hydrogen release of 7.7 wt% after 8 h. Compared to the theoretical value of 7.75 wt%, the relative error of the measurement was only 0.64%, demonstrating the high accuracy of the calibration and analytical method.

Based on a propagation-of-uncertainty analysis and typical operating conditions (2.1 MPa and 350 °C), the relative contributions of pressure (±0.05 bar) and temperature (±1 K) uncertainties were 0.24% and 0.16%, respectively. When combined with the uncertainties associated with volumetric calibration (~1%) and compressibility factor estimation (~0.1%), the total relative uncertainty in the absorbed hydrogen amount was estimated to be approximately 1.0–1.1%. Therefore, the overall experimental uncertainty of the developed system remains close to 1% and well below 2%, comparable to, and in some cases better than, values reported for commercial Sieverts-type apparatuses.

Fig. 4 shows the Temperature-Programmed Desorption (TPD) curves for the MgH_2–1 wt% C@Ni sample, obtained at a heating rate of 5 °C/min. The onset temperature for dehydrogenation is observed at approximately 275 °C, which is about 45 °C lower than that of the sample without carbon-coated nickel addition (321 °C, cf. [19]). Fig. 5 presents the isothermal hydrogen desorption and absorption kinetic curves for the composite at 350 °C, 300 °C, and 275 °C. For desorption, the samples at 350 °C and 300 °C achieved maximum hydrogen release of −6.54 wt% and −6.50 wt%, respectively, at 5 min and 12 min. In contrast, the desorption curve at 275 °C exhibits a less pronounced asymptotic trend, reaching −4.14 wt% after 40 min. In the absorption experiments, the hydrogen uptake values for 300 °C and 275 °C were similar, measuring 6.0 wt% and 6.08 wt%, respectively. At 350 °C, the sample achieved a higher hydrogen content of 6.63 wt%, with over 97% of the total hydrogen absorbed within the first minute, demonstrating remarkably fast kinetics. Details of the calculation procedures and data analysis for these curves are available in the Python notebook "Kinetic_MgH_2-1wtC@Ni.ipynb", accessible via the provided link.

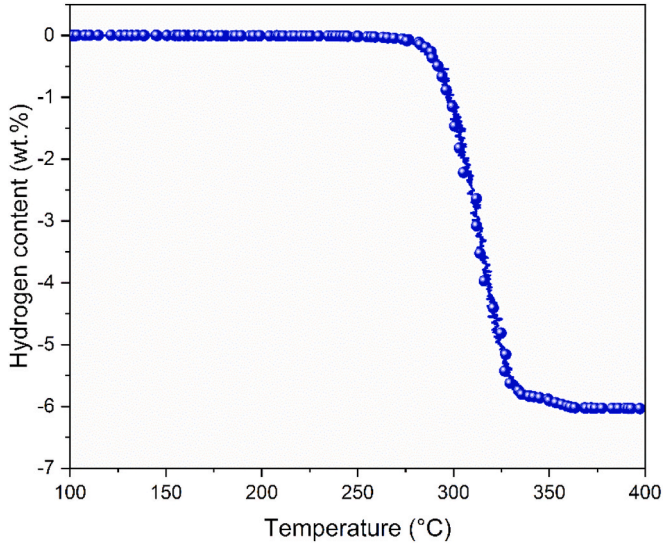

Fig. 4. Temperature-Programmed Desorption (TPD) curves at 5 °C/min of MgH_2 – 1 wt% C@Ni.

Fig. 6 presents the pressure–composition isotherm (PCI) for the sample measured at 350 °C, revealing an equilibrium plateau pressure of approximately 0.65 MPa during both absorption and desorption. The isotherm exhibits a well-defined plateau with negligible hysteresis between absorption and desorption branches. The maximum hydrogen storage capacity achieved at this temperature was 6.85 wt%, in agreement with both the previously reported kinetic results and literature values for Mg-based hydrides under similar conditions.

Details of the calculation procedures and data analysis for these isotherms are provided in the Python notebook "PCI-350_MgH_2-1wtC@Ni.ipynb". After 10 absorption/desorption cycles at 350 °C, the sample maintained a reversible hydrogen desorption capacity of 6.04 wt% (representing a retention of 92%), while the reversible hydrogen absorption capacity remained at 5.96 wt% (90% retention). These results demonstrate good cycling stability of the composite material. The computational workflow and analysis for these cycling tests are presented in the Python notebook "Cycles-350_MgH_2-1wtC@Ni.ipynb".

Fig. 7 presents the graphical representation of the ten consecutive cycles performed on the MgH_2–1wt% C@Ni composite. In contrast, Fig. 8 shows the results obtained for $LaNi_5$, where the measurement system was subjected to repeated cycling over 70 consecutive kinetic absorption/desorption tests. In this case, a progressive improvement in hydrogen storage capacity is observed as a result of the activation effect induced by cycling, reaching values close to 1.4 wt% hydrogen content. These results further demonstrate the stability, reproducibility, and operational reliability of the automated Sieverts-type system under extended cyclic loading and with hydrides of different thermodynamic and kinetic characteristics.

Over the course of PCI and Cycles experiments, the PCD executed more than 100 automatic dosing events, seamlessly adjusting to each programmed pressure step in the experimental sequence. At each event, the PCD rapidly stabilized the system pressure to the target setpoint, minimizing equilibration time and ensuring consistent, controlled gas delivery.

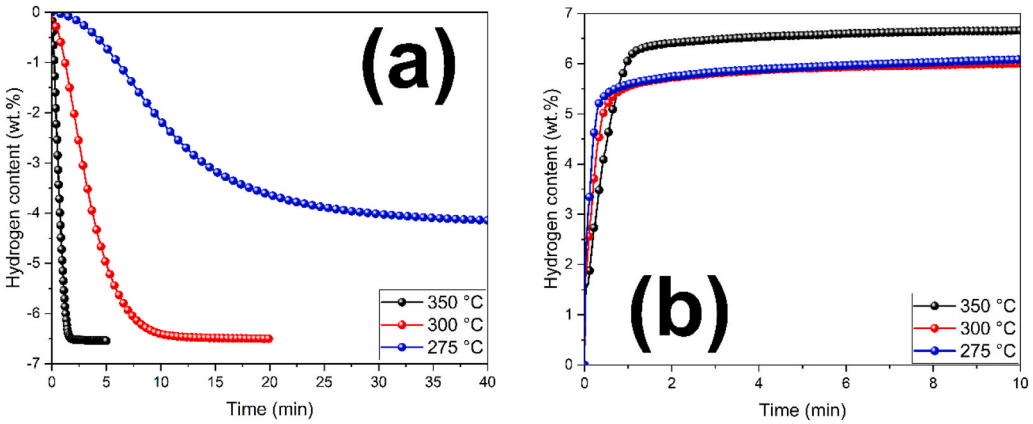

Fig. 5. Isothermal hydrogen desorption kinetics curves of the sample at 350 °C, 300 °C, and 275 °C (a). Isothermal hydrogen absorption kinetics curves of the samples at 350 °C, 300 °C, and 275 °C (b).

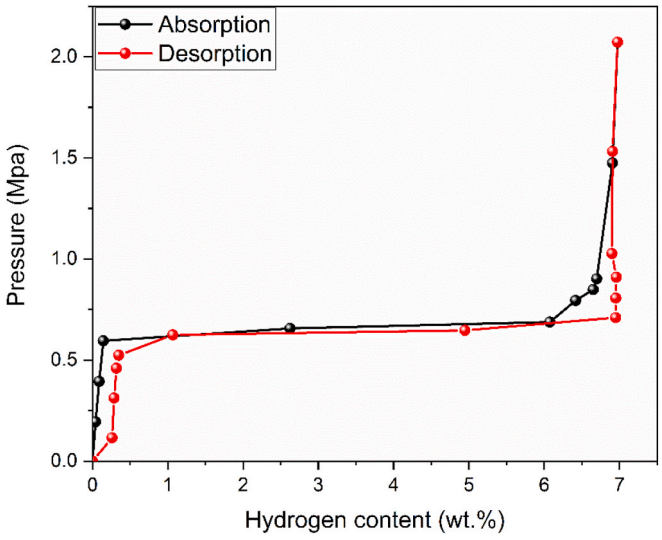

Fig. 6. Pressure-Composition Isotherm curve in absorption/desorption of the sample at 350 °C.

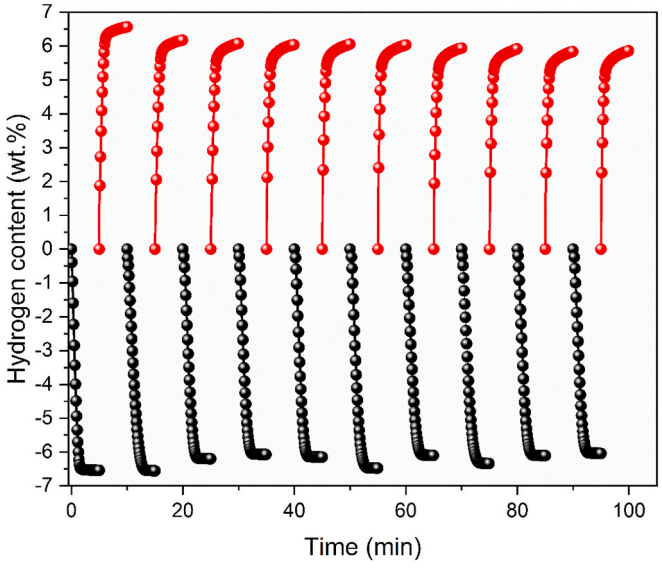

Fig. 7. Hydrogen desorption/absorption cycles plot at 350 °C of MgH_2 - 1 wt % C@Ni.

6. Discussion

A detailed comparison with previously reported self-built Sieverts-type apparatuses, summarized in Table 1, highlights clear architectural and functional differences between the present system and earlier designs. Most reported setups rely on relatively simple pressure regulation strategies, including pneumatic on/off valves combined with needle valves [5,16], mass flow controllers [6], piston pumps [7], or high-pressure regulators with limited automation details [15]. In several cases, programmable pressure steps are mentioned but not explicitly described in terms of hardware implementation or control logic [4,14,17]. More recent compact designs incorporate gas bottles and enlarged volumes for automated dosing but remain largely dedicated to PCI analysis and lack general-purpose flexibility [3,18]. In contrast, the system proposed in this work integrates a dual-valve pressure control device (PCD) within a PLC–Python architecture, enabling fine, stepwise, and fully automated pressure dosing over a wide operating range. This approach provides precise control of pressure ramps, stable setpoint maintenance, and reproducible multi-step dosing sequences for calibration, PCI, kinetics, and cycling experiments within a single unified framework. Furthermore, the modular layout and digital integration of the PCD allow seamless extension toward adaptive and feedback-based dosing strategies, which are not reported in the self-constructed systems reviewed. These features promote advances in automation level, operational versatility, and pressure-control sophistication in self-built Sieverts-type instruments.

A relevant aspect of the present work is the cost–performance balance of the developed system in comparison with a commercial Sieverts-type apparatus. Commercial high-pressure Sieverts analyzers, such as the BSD PH series from BSD Instruments (China) and the iSorb system from Quantachrome/Anton Paar (USA), typically range between 85,000 and 160,000 USD based on quotations obtained prior to the construction of the present setup. In contrast, the total material and component cost of the self-built system reported here was approximately 20,000 USD, representing a substantial reduction in capital investment. This comparison does not include the non-monetary cost associated with system design, development, and optimization, which required nearly two years of interdisciplinary work; however, this effort also provided significant added value in terms of in-house expertise, flexibility, and system understanding. Regarding long-term operation, annual maintenance costs are estimated to be on the order of 5000 USD, mainly associated with consumables and replacement components such as VCR gasket seals, tubing, nuts, ferrules, ball valve or bellows kits, anti-seize compounds, and fittings (e.g., tees and crosses) required to address minor leaks or routine wear. These operational costs are comparable to those of commercial systems and are inherent to high-pressure hydrogen installations. Overall, the results demonstrate that a self-built Sieverts-

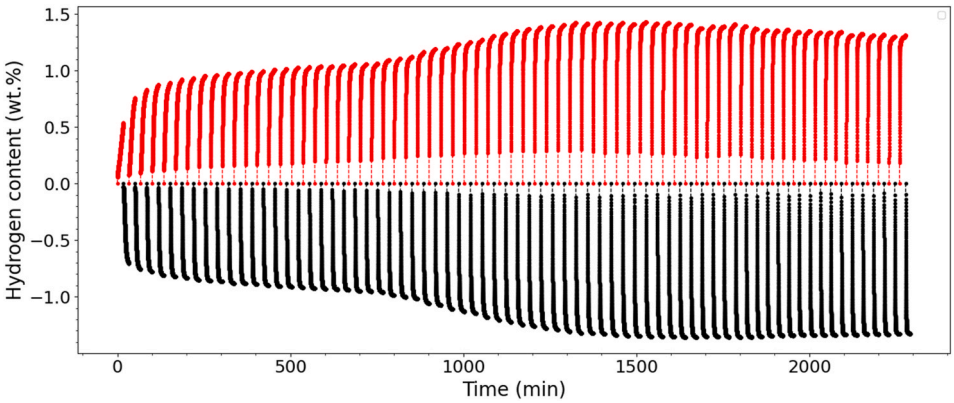

Fig. 8. Hydrogen desorption/absorption cycles plot at 25 °C of $LaNi_5$.

type apparatus can achieve competitive performance at a fraction of the acquisition cost of commercial equipment, while offering high adaptability and significant educational and technological benefits.

During calibration, the PCD efficiently facilitated the consecutive dosing required for the 25 expansion cycles that compose the volume calibration procedure. Analysis of the V_{sc}/V_{ref} ratios across different temperature data sets revealed a low standard deviation, reflecting high consistency and reproducibility of the method. Because the sample and reference cell volumes were calculated relative to a third, known volume, the two unknown volumes are expressed as ratios to the calibrated volume and thus inherently correlated. This approach has been shown to yield superior accuracy compared to separate volume determinations. In particular, Webb and MacA Gray (2014, [21]) emphasize that carefully executed measurements involving both known volumes and the two unknown volumes simultaneously can achieve highly accurate calibrations. In our system, this precision was facilitated by the programmable flexibility and rapid, accurate pressure adjustments enabled by the PCD.

To validate the absolute volume determinations, we compared the maximum hydrogen desorption capacity measured for $LiAlH_4$ with established literature values. The observed sequential hydrogen release (approximately 5.2–5.3 wt% between 150 and 175 °C, 2.4–2.6 wt% from 180 to 220 °C, and an additional 2.6 wt% at temperatures above 400 °C [22,23]), closely matched reported values. The minimal relative error in this comparison confirms the accuracy of our calibration method across multiple thermal decomposition steps of $LiAlH_4$.

Regarding the sample used to validate common measurement procedures with Sieverts-type equipment, the dehydrogenation onset temperature was observed at approximately 275 °C, which is about 45 °C lower than that of the undoped sample [19]. This significant reduction indicates a marked improvement in hydrogen release kinetics attributable to the addition of carbon-coated nickel nanoparticles (C@Ni). Since 2024, our research group has been publishing studies on magnesium thin flakes [24] and magnesium hydrides, particularly exploring their synergistic effects with nickel and titanium dopants [19,25]. The material analyzed in this work belongs to a family of composites recently published, which emphasized the accessibility of raw materials and the relatively simple simultaneous grinding and mixing process of sample preparation [19]. That prior study demonstrated promising enhancements in hydrogen storage capacity and kinetics for magnesium hydride samples with comparable particle size distributions doped with commercial C@Ni nanoparticles.

While the current measurements for TPD, kinetics, and cycling tests were not previously reported, they can be objectively compared to this earlier work, which investigated different milling protocols and C@Ni concentrations (10, 5, 3, and 0.5 wt%). The material selected for this study was chosen based on those prior results with clear expectations regarding its performance. Our findings are consistent with those earlier observations, reaffirming that pronounced particle size refinement and homogeneous nanoparticle dispersion significantly enhance interfacial contact and improve the hydrogen storage properties of the composite, specially at low C@Ni weight fractions. A more comprehensive discussion of the material's advantages and related mechanisms can be found in the aforementioned publication.

Regarding the PCI measurements, the isotherm displays a well-defined plateau characteristic of the Mg ↔ MgH_2 phase transition, with minimal hysteresis between absorption and desorption branches, a behavior commonly observed at elevated temperatures. For pure or nanostructured Mg materials at 350 °C, equilibrium hydrogen pressures for the absorption plateau generally range from approximately 0.6 to 1.2 MPa, with hydrogen storage capacities approaching the theoretical maximum of about 7.6 wt% for MgH_2. Nanoscale structuring and doping often cause slight variations in plateau pressure and capacity due to modified thermodynamics and enhanced kinetics. Specifically, bulk Mg typically exhibits an absorption plateau near 1.0 MPa at 350 °C, whereas nanostructured or catalytically modified samples often demonstrate reduced plateau pressures owing to altered phase stability and improved reaction rates [26,27].

The measured plateau pressure in this work aligns well with these reported trends, reflecting the expected decrease due to nanoscaling or alloying effects, while the overall two-phase isotherm shape remains consistent. When combined with isotherms collected at other temperatures, these curves will enable the extraction of key thermodynamic parameters essential for modeling and designing hydrogen storage systems based on this material.

Pure MgH_2 typically exhibits poor cyclability, with capacity retention often falling below 70% [28,29]. The addition of nickel-based additives has been shown to significantly improve cyclability, achieving retention values above 95% in some cases [30,31]. The 92% capacity retention observed in this study aligns well with these improved values reported in the literature for MgH_2 doped with nickel additives, though it is noted that such additives do not always guarantee enhanced cycling stability [32]. A similar behavior was observed in the cycling stability tests performed with $LaNi_5$. Typical reversible hydrogen storage capacities for $LaNi_5$ are in the range of 1.3–1.5 wt%, while well-activated kinetic tests commonly reach ~1.2–1.3 wt% within a few minutes. In the present study, absorption and desorption truncation times of 18 and 16 min, respectively, were consistently observed during cycling, indicating rapid kinetics and effective activation of the material. The stabilization of hydrogen capacity close to 1.4 wt% after repeated cycling further confirms the expected activation effect and demonstrates the capability of the developed system to reliably capture fast kinetic responses and subtle capacity evolution in low-temperature hydrides.

Traditional pressure–composition isotherm (PCI) measurements require gradually increasing hydrogen pressure while maintaining a constant temperature and allowing sufficient equilibration time at each step. The PCD streamlines this process by continuously and precisely

adjusting the hydrogen pressure in programmed increments and automatically controlling dwell times to ensure equilibrium is reached, thereby substantially reducing the need for manual intervention. This level of automation improves data resolution within critical plateau regions, enhances measurement repeatability, and minimizes human error and operator dependency—challenges often encountered in self-built Sieverts-type systems.

Furthermore, the PCD's capacity to execute complex dosing sequences and rapidly respond to real-time system feedback guarantees stable and reliable operation during extended PCI and cyclic absorption/desorption protocols. This not only improves the accuracy and reproducibility of thermodynamic data from PCI tests but also ensures consistent control during repeated cycling, which is essential for evaluating the material's hydrogen storage stability. Notably, no malfunctions or operational anomalies were recorded throughout the extended series of automated steps.

The consistent results obtained in this study validate the robustness of our measurement approach, confirming both the experimental setup's reliability and the reproducibility of the material's performance under rigorous testing conditions.

7. Conclusions

This study successfully documented and tested the integration of a dual-valve Pressure Control Device (PCD) into a self-built Sieverts-type apparatus, significantly enhancing automation, precision, and operational efficiency in hydrogen storage measurements. The PCD enabled fully automated pressure dosing and venting during volume calibration, thermal-programmed desorption (TPD), absorption/desorption kinetics, pressure–composition isotherm (PCI) determination, and cyclic stability tests, substantially reducing manual intervention and minimizing measurement variability. This advancement provides a cost-effective and scalable solution that enhances existing systems by bridging the gap toward high-end commercial apparatuses. It effectively overcomes typical limitations in accessibility and flexibility while ensuring reliable and reproducible data acquisition, an essential factor for advancing hydrogen storage research.

Experimentally, the system was validated for calibration using dehydrogenation of $LiAlH_4$, and for common measurement procedures with Sieverts-type apparatuses, magnesium hydride doped with 1 wt% carbon-coated nickel nanoparticles was used, which exhibited improved hydrogen sorption characteristics, including a lowered dehydrogenation onset temperature, rapid kinetics, and a stable hydrogen capacity of 6.85 wt% at 350 °C. The material showed excellent cyclic performance, retaining 92% of its capacity after 10 absorption/desorption cycles. The precise and responsive control provided by the pressure control device (PCD) over 25 automated dosing steps during calibration, 31 steps during PCI measurements, and up to 80 steps in cycling experiments was critical to achieving high-quality, repeatable, and reliable results. In addition to the study conducted with the magnesium-based composite, extended cycling tests with a higher number of repetitions were performed on low-temperature hydrides such as $LaNi_5$, in order to demonstrate the applicability and versatility of the instrumentation across different classes of hydrogen storage materials. Overall, this work highlights both instrumental and material advances that together contribute to the development of solid-state hydrogen storage technologies and support the advancement of sustainable energy solutions.

CRediT authorship contribution statement

Julián Arias: Writing – original draft, Visualization, Validation, Software, Methodology, Formal analysis, Data curation, Conceptualization. **Robinson Aguirre Ocampo:** Visualization, Validation, Methodology, Conceptualization. **Joan Santiago Cortinez:** Validation, Methodology. **Carlos Arrieta:** Supervision, Resources, Project administration, Investigation, Funding acquisition, Formal analysis, Conceptualization. **Francisco Bolivar:** Project administration, Investigation, Funding acquisition. **Alejandro Zuleta:** Investigation, Funding acquisition. **José A. Tamayo:** Methodology, Investigation, Funding acquisition, Conceptualization. **Andrés F. Vargas:** Methodology, Funding acquisition, Conceptualization. **Esteban Correa:** Project administration, Methodology, Investigation, Funding acquisition, Conceptualization. **Félix Echeverria:** Writing – review & editing, Validation, Supervision, Resources, Project administration, Methodology, Investigation, Funding acquisition, Formal analysis, Conceptualization.

Declaration of generative AI and AI-assisted technologies in the writing process

During the preparation of this work, the authors utilized Prerplexity Pro to assist with language refinement and proofreading, specifically to enhance fluency and comprehensibility, as well as to refine certain sections of the manuscript. After using this tool, the authors reviewed and edited the content as needed and take full responsibility for the content of the publication.

Declaration of competing interest

The authors declare that they have no known competing financial interests or personal relationships that could have appeared to influence the work reported in this paper.

8. Acknowledgements

The authors gratefully acknowledge the technical contributions of the Master's student, Alejandro Gomez, and the Eng. Andrés Pérez during the device's development. Financial support was provided by the Sistema General de Regalías (SGR) through project BPIN 2022000100089; the Ministry of Science, Technology and Innovation (Minciencias) through project 69950, "*Aplicación de la nanotecnología al desarrollo de materiales basados en magnesio para almacenamiento de hidrógeno, con el fin de contribuir a viabilizar su uso como combustible limpio en sistemas de transporte*"; the "*Estrategia de Sostenibilidad de la Universidad de Antioquia*"; the Centro de Investigación para el Desarrollo de la Innovación (CIDI), Universidad Pontificia Bolivariana (Rad: 822C-06/23-35); and the Centro de Investigación en Ingenierías (CEIN), Universidad de Medellín.

Appendix A. Supplementary data

Supplementary data to this article can be found online at https://doi.org/10.1016/j.ijhydene.2026.154042.

References

[1] Canjura Rodriguez P, Gallandat N, Züttel A. Accurate measurement of pressure-composition isotherms and determination of thermodynamic and kinetic parameters of metal hydrides. Int J Hydrogen Energy 2019;44:13583–91. https://doi.org/10.1016/J.IJHYDENE.2019.03.224.

[2] Weinberger B, Lamari FD. High pressure cryo-storage of hydrogen by adsorption at 77K and up to 50MPa. Int J Hydrogen Energy 2009;34:3058–64. https://doi.org/10.1016/j.ijhydene.2009.01.093.

[3] Zhu H, Zhou D, Chen D, Cheng H. Design of ultra-efficient and automatically temperature-variable cycle (TVC) sieverts apparatus for testing sorption properties of hydrogen storage materials. Int J Hydrogen Energy 2024;62:172–85. https://doi.org/10.1016/j.ijhydene.2024.03.018.

[4] Zielinski JM, Coe CG, Nickel RJ, Romeo AM, Cooper AC, Pez GP. High pressure sorption isotherms via differential pressure measurements. Adsorption 2007;13:1–7. https://doi.org/10.1007/s10450-007-9005-9.

[5] Lim KL, Chan SLI, Yang R, Li S. Hydrogen storage alloys for remote area power supply. Australia: UNSW; 2015. https://doi.org/10.26190/unsworks/17397.

[6] Policicchio A, Maccallini E, Kalantzopoulos GN, Cataldi U, Abate S, Desiderio G, et al. Volumetric apparatus for hydrogen adsorption and diffusion measurements: sources of systematic error and impact of their experimental resolutions. Rev Sci Instrum 2013;84:103907. https://doi.org/10.1063/1.4824485.

[7] Pyle DS, Gray EMA, Webb CJ. A sieverts apparatus for measuring high-pressure hydrogen isotherms on porous materials. Int J Hydrogen Energy 2017;42:20111–9. https://doi.org/10.1016/J.IJHYDENE.2017.06.126.
[8] Ribeiro ES, Gil JM. Instrumentation and characterization of materials for hydrogen storage. Ciência Tecnol Dos Mater 2016;28:99–105. https://doi.org/10.1016/J.CTMAT.2017.01.002.
[9] Blach TP, Gray EM. Sieverts apparatus and methodology for accurate determination of hydrogen uptake by light-atom hosts. J Alloys Compd 2007;446–447:692–7. https://doi.org/10.1016/j.jallcom.2006.12.061.
[10] Chen Y, Liu Q, Yan Y, Cheng X, Liu Y. Influence of sample cell physisorption on measurements of hydrogen storage of carbon materials using a sieverts apparatus. Carbon N Y 2010;48:714–20. https://doi.org/10.1016/J.CARBON.2009.10.016.
[11] Gray EMA, Webb CJ. Performance analysis of a sieverts apparatus for measuring hydrogen uptake. Int J Hydrogen Energy 2022;47:14628–36. https://doi.org/10.1016/J.IJHYDENE.2022.02.196.
[12] Carrillo-Bucio JL, Tena-Garcia JR, Armenta-Garcia EP, Hernandez-Silva O, Cabañas-Moreno JG, Suárez-Alcántara K. Low-cost Sieverts-type apparatus for the study of hydriding/dehydriding reactions. HardwareX 2018;4:e00036. https://doi.org/10.1016/j.ohx.2018.e00036.
[13] Meyer G, Arneodo Larochette P, Baruj A, Castro FJ, Lacharmoise P, Zacur E, et al. Equipment for hydrogen absorption-desorption cycling characterization of hydride forming materials. Rev Sci Instrum 2007;78:23903. https://doi.org/10.1063/1.2437160.
[14] Talagañis BA, Castro FJ, Baruj A, Meyer G. Novel device for simultaneous volumetric and x-ray diffraction measurements on metal-hydrogen systems. Rev Sci Instrum 2009;80:73901. https://doi.org/10.1063/1.3157086.
[15] Voskuilen T, Zheng Y, Pourpoint T. Development of a sievert apparatus for characterization of high pressure hydrogen sorption materials. Int J Hydrogen Energy 2010;35:10387–95. https://doi.org/10.1016/j.ijhydene.2010.07.169.
[16] Ceteroni I. High-pressure adsorption differential volumetric apparatus (HP-ADVA) for accurate equilibrium measurements [Master's thesis]. Bologna (Italy): Universitá di Bolognia; 2020.
[17] Testi M, Bartali R, Crema L. Design and optimization of Isochoric Differential apparatus (IDA) to reduce uncertainty in H2 sorption process measurements. Int J Hydrogen Energy 2020;45:10775–96. https://doi.org/10.1016/J.IJHYDENE.2020.01.190.
[18] Zhu H, Cheng H, Chen D, Ding Z. Development of compact and efficient volumetric apparatus for measuring absorption/desorption properties of hydrogen storage materials. Int J Hydrogen Energy 2022;47:32565–81. https://doi.org/10.1016/j.ijhydene.2022.07.148.
[19] Ocampo RA, Arias-Velandia J, Lenis JA, Zuleta Gil AA, Bello S, Correa E, et al. Catalytic effect of commercial carbon-coated nickel nanoparticles on the hydrogen storage performance of magnesium hydride. Int J Hydrogen Energy 2025;129:91–100. https://doi.org/10.1016/j.ijhydene.2025.04.226.
[20] Gross KJ, Carrington KR, Barcelo S, Karkamkar A, Purewal J, Ma S, et al. Recommended best practices for the characterization of storage properties of hydrogen storage materials. EMN-HYMARC (EMN-HyMARC). Golden, CO: National Renewable Energy Lab.(NREL); 2016.
[21] Webb CJ, Gray EM. The effect of inaccurate volume calibrations on hydrogen uptake measured by the sieverts method. Int J Hydrogen Energy 2014;39:2168–74. https://doi.org/10.1016/j.ijhydene.2013.11.121.
[22] Ahmad MAN, Sazelee NA, Ali NA, Ismail M. Enhancing the dehydrogenation properties of LiAlH4 using K2NiF6 as additive. Int J Hydrogen Energy 2022;47:24843–51. https://doi.org/10.1016/j.ijhydene.2022.05.224.
[23] Ares Fernandez JR, Aguey-Zinsou F, Elsaesser M, Ma XZ, Dornheim M, Klassen T, et al. Mechanical and thermal decomposition of LiAlH4 with metal halides. Int J Hydrogen Energy 2007;32:1033–40. https://doi.org/10.1016/j.ijhydene.2006.07.011.
[24] Cortinez JS, Gómez A, Zuleta Gil AA, Tamayo JA, Correa E, Bolívar FJ, et al. Production of Mg thin flakes with enhanced hydrogen storage performance. Int J Hydrogen Energy 2024;71:1191–200. https://doi.org/10.1016/j.ijhydene.2024.05.254.
[25] Cortínez JS, Gómez A, Zuleta AA, Tamayo JA, Correa E, Bolívar FJ, et al. Improved hydrogen storage in magnesium thin flakes via nickel and titanium/titanium carbide additives. Int J Hydrogen Energy 2025;153:150264. https://doi.org/10.1016/j.ijhydene.2025.150264.
[26] Baran A, Polański M. Magnesium-based materials for hydrogen Storage-A scope review. Mater (Basel, Switzerland) 2020;13. https://doi.org/10.3390/ma13183993.
[27] Li B, Li J, Shao H, He L. Mg-Based hydrogen absorbing materials for thermal energy storage—A review. Appl Sci 2018;8. https://doi.org/10.3390/app8081375.
[28] Peng C, Li Y, Zhang Q. Enhanced hydrogen desorption properties of MgH2 by highly dispersed Ni: the role of in-situ hydrogenolysis of nickelocene in ball milling process. J Alloys Compd 2022;900:163547. https://doi.org/10.1016/j.jallcom.2021.163547.
[29] Tan D, Peng C, Zhang Q. Microstructural characteristics and hydrogen storage properties of the Mg–Ni–TiS2 nanocomposite prepared by a solution-based method. Int J Hydrogen Energy 2023;48:16756–68. https://doi.org/10.1016/j.ijhydene.2023.01.185.
[30] Yuan Q, Peng C, Yang C, Li Y, Zhang Q, Lv Y, et al. Facilitated hydrogen storage properties of MgH2 by Ni nanoparticles anchored on Mo2C@C nanosheets. Int J Hydrogen Energy 2024;85:12–9. https://doi.org/10.1016/j.ijhydene.2024.08.292.
[31] Wang Z, Tian Z, Yao P, Zhao H, Xia C, Yang T. Improved hydrogen storage kinetic properties of magnesium-based materials by adding Ni2P. Renew Energy 2022;189:559–69. https://doi.org/10.1016/j.renene.2022.03.001.
[32] Tome KC, Xi S, Fu Y, Lu C, Lu N, Guan M, et al. Remarkable catalytic effect of Ni and ZrO2 nanoparticles on the hydrogen sorption properties of MgH2. Int J Hydrogen Energy 2022;47:4716–24. https://doi.org/10.1016/j.ijhydene.2021.11.102.